

ϕ -Meson Production in e^+e^- Annihilations at 29 GeV

H. Aihara, M. Alston-Garnjost, D. H. Badtke, J. A. Bakken, A. Barbaro-Galtieri, B. A. Barnett, A. V. Barnes, B. J. Blumenfeld, A. D. Bross, C. D. Buchanan, O. Chamberlain, J. Chiba, C.-Y. Chien, A. R. Clark, A. Cordier, O. I. Dahl, C. T. Day, K. A. Derby, P. H. Eberhard, D. L. Fancher, H. Fujii, T. Fujii, B. Gabioud, J. W. Gary, W. Gorn, N. J. Hadley, J. M. Hauptman, H. J. Hilke, W. Hofmann, J. E. Huth, J. Hylen, H. Iwasaki, T. Kamae, R. W. Kenney, L. T. Kerth, R. I. Koda, R. R. Kofler, K. K. Kwong, J. G. Layter, C. S. Lindsey, S. C. Loken, X.-Q. Lu, G. R. Lynch, L. Madansky, R. J. Madaras, R. M. Majka, P. S. Martin, K. Maruyama, J. N. Marx, J. A. J. Matthews, S. O. Melnikoff, W. Moses, P. Nemethy, D. R. Nygren, P. J. Oddone, D. A. Park, A. Pevsner, M. Pripstein, P. R. Robrish, M. T. Ronan, R. R. Ross, F. R. Rouse, R. R. Sauerwein, G. Shapiro, M. D. Shapiro, B. C. Shen, W. E. Slater, M. L. Stevenson, D. H. Stork, H. K. Ticho, N. Toge, R. F. van Daalen Wetters, G. J. VanDalen, R. van Tyen, H. Videau, M. R. Wayne, W. A. Wenzel, H. Yamamoto, M. Y. Yamauchi, M. E. Zeller, and W.-M. Zhang

Lawrence Berkeley Laboratory, University of California, Berkeley, California 94720, and University of California, Los Angeles, California 90024, and University of California, Riverside, California, 92521, and Johns Hopkins University, Baltimore, Maryland 21218, and University of Massachusetts, Amherst, Massachusetts 01003, and University of Tokyo, Tokyo 113, Japan, and Yale University, New Haven, Connecticut 06520

(Received 3 April 1984)

Production of ϕ mesons in e^+e^- annihilation at a center-of-mass energy of 29 GeV has been observed with the time-projection chamber detector at the PEP storage ring. The ϕ production rate has been measured in the energy range $0.075 < x < 0.55$ ($x = 2E_\phi/\sqrt{s}$), giving $0.077 \pm 0.012(\text{stat}) \pm 0.016(\text{syst})$ ϕ 's per event. The average value of p_t^2 relative to the thrust axis is 1.0 ± 0.4 (GeV/c)².

PACS numbers: 13.65.+i, 14.40.Cs

The investigation of resonance production in electron-positron (e^+e^-) annihilation at high energies provides important information on the mechanism of parton fragmentation. While high-statistics inclusive data on final-state stable hadrons have been reported,¹⁻³ their interpretation in terms of parton fragmentation is hindered by the fact that the shapes of the spectra may be dominated by decay products of heavier particles. The behaviors of resonances⁴ are, on the other hand, more directly related to the quantum number and energy flow of the original partons and their hadronization.

We have measured the inclusive ϕ production in e^+e^- annihilation at a center-of-mass energy of 29 GeV. The data were collected with the PEP-4 time-projection chamber (TPC) detector at the PEP storage ring. The TPC was used to identify kaons by dE/dx and to reconstruct the decay $\phi \rightarrow K^+K^-$. The apparatus, monitoring, calibration, and event selection have been described elsewhere.^{3,5} The results presented here are based on a sample of 25 900 hadronic events, corresponding to an integrated luminosity of 69 pb^{-1} .

In this analysis all reconstructed tracks in the TPC are required to meet the following conditions: (1) the distance of closest approach to the average

incident beam-beam interaction point is smaller than 3 cm in the plane transverse to the beam and smaller than 5 cm along the beam, (2) $|\cos\theta| < 0.84$, where θ is the polar angle of the track relative to the beam, (3) the momentum p is larger than 0.15 GeV/c, (4) the estimated error in the momentum measurement satisfies either $dp_{xy}/p_{xy} < 0.3$ or $dp_{xy}/p_{xy}^2 < 0.3$ (GeV/c)⁻¹, where p_{xy} is the momentum component transverse to the beam. These cuts reduce contributions from nuclear interactions and photon conversions in the material in front of the TPC.

The charged-particle species were identified by a simultaneous measurement of the momentum and of up to 183 samples of dE/dx ionization energy loss. We define dE/dx for each track to be the mean of the smallest 65% of the individual samples. On the average 110 dE/dx samples are used per track in multihadronic events, giving a typical dE/dx resolution of 3.7%. The momentum resolution was $(dp/p)^2 \simeq (0.06)^2 + (0.035p)^2$.

From the measured dE/dx and momentum for each particle, χ^2 values for $e/\pi/K/p$ hypotheses are calculated using an empirically determined formula to relate dE/dx to particle momentum. The parameters in this formula have been established by

measuring minimum ionizing particles, cosmic-ray muons, and Bhabha electrons. Then weights are defined for the $e/\pi/K/p$ hypotheses as

$$W(i) = f(i,p) \exp[-\chi(i)^2/2]/N,$$

where $i = e, \pi, K, p$, $f(i,p)$ is the particle fraction of particle type i measured at momentum p in the hadronic event sample,³ and N is a normalization factor to ensure that $W(e) + W(\pi) + W(K) + W(p) = 1$. A track is counted as one kaon if it satisfies $W(K) > 0.7$. The purity of the kaon sample selected in this way is about 70% and nearly constant over the entire momentum range. The momentum-dependent acceptance for kaons is typically 50%. It is particularly small (10%–15%) in the range $0.9 < p < 1.5$ GeV/c, where π and K bands overlap in the dE/dx versus momentum plane. This is because $W(K)$ is reduced by the large value of $f(\pi)$ relative to $f(K)$.

Figure 1(a) shows the K^+K^- invariant-mass distribution in the range $0.075 < x < 0.55$, where

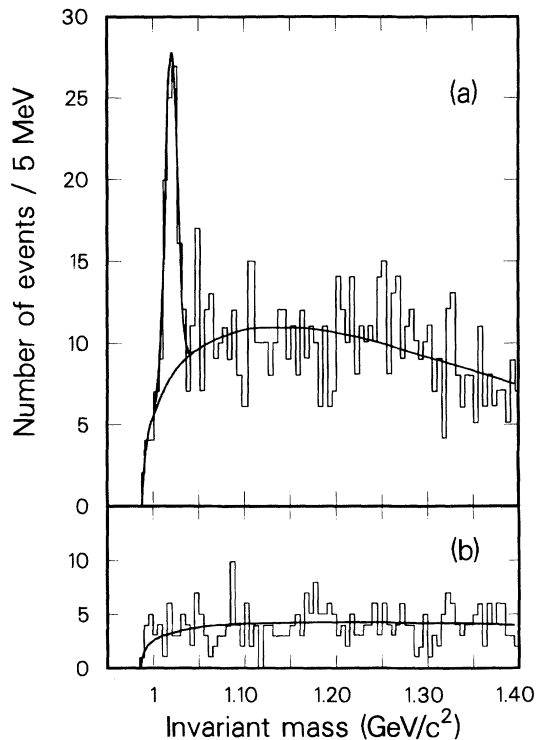


FIG. 1. (a) K^+K^- invariant-mass spectrum in the energy range $0.075 < x < 0.55$, where $x = 2E/\sqrt{s}$. The fitted curve includes a Gaussian line shape plus a background whose shape has been obtained by Monte Carlo and parametrized as a smooth function. (b) Sum of K^+K^+ and K^-K^- invariant-mass spectra. The smooth curve shows a Monte Carlo prediction of the spectrum.

$x = 2E(K^+K^-)/\sqrt{s}$, and $E(K^+K^-)$ is the sum of two kaon energies. A clear peak is observed in the ϕ mass region just above the K^+K^- threshold. No such structure is seen in the like-sign combinations of kaons, as shown in Fig. 1(b). Contributions from photon conversion pairs, K_S^0 decays, and other resonances, whose products are taken to be kaons, are estimated to be small [less than two entries in $1.00 < M(K^+K^-) < 1.05$ GeV] and flat, so that they cannot contribute to the sharp peak in the ϕ region.⁶ Fitting the distribution in Fig. 1(a) with a Gaussian line shape plus a smooth background gives 62.2 ± 10.5 entries in the peak, $M(K^+K^-) = 1.019 \pm 0.002$ GeV, and root-mean-square width $= 6.2 \pm 0.4$ MeV, which is consistent with the estimated detector resolution for $\phi \rightarrow K^+K^-$. Thus, we attribute the peak in Fig. 1(a) to ϕ production.

The detection efficiencies are evaluated with a Monte Carlo calculation which generates multihadron events with initial-state radiative corrections,⁷ and an analysis procedure identical to that used for the data. The simulation of the detector includes geometrical acceptance, track-pattern recognition, decay loss of pions and kaons, particle energy loss in the material, multiple scattering, nuclear interactions, loss of dE/dx wire samples due to overlapping tracks, and its effect on the dE/dx resolution. The estimates of the particle identification efficiencies and purities were checked in two ways for consistency. First, using particle identities determined by imposing various cuts on $W(\pi)$, $W(K)$, and $W(p)$ for tracks in multihadron events, we observed that the numbers of $\pi/K/p$'s, corrected for purities and efficiencies, lead to results consistent with those reported in Ref. 3. Second, using low-energy electrons and positrons from conversion pairs in Bhabha events, we found that the numbers of electrons and positrons misidentified as π , K , or p agree with predictions from the Monte Carlo.

We searched for signatures of spin alignment of the observed ϕ 's by looking at decay angular distributions in the ϕ rest frame. We tried two helicity axes: (a) the flight direction of ϕ 's, and (b) the line perpendicular to the plane determined by the event thrust axis and the ϕ flight direction. For various angle and energy intervals, K^+K^- invariant-mass spectra were fitted with combinations of a Gaussian peak and a background term. Then the number of entries in each peak, corrected for the ϕ detection efficiency, was fitted with a curve $(1 + \alpha \cos^2 \theta_{KK})$, where θ_{KK} is the ϕ decay angle with respect to one of the reference axes defined above. In the region integrated over 0.075

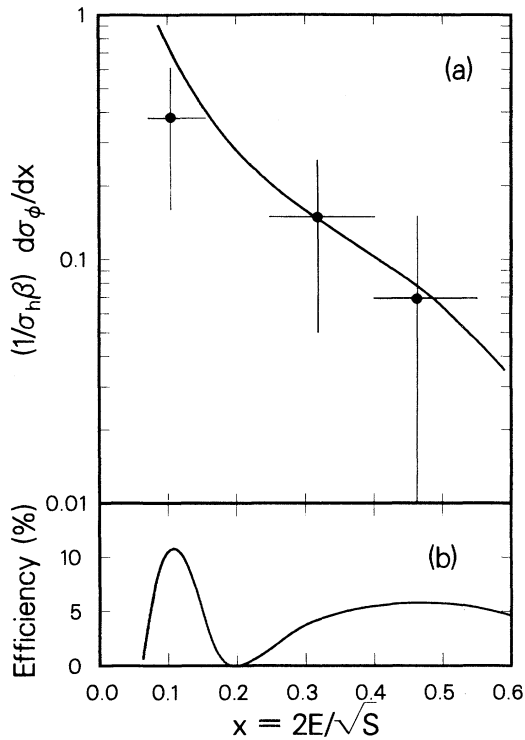


FIG. 2. (a) ϕ inclusive cross section as a function of $x = 2E_\phi/\sqrt{s}$. The solid curve shows a prediction of the Lund model, obtained with parameters $s/u=0.3$, $V/(V+P)=0.5$. (b) ϕ detection efficiency as a function of x , including the $\phi \rightarrow K^+K^-$ branching fraction and initial-state radiative corrections.

$< x < 0.55$, we obtained $\alpha = -0.01 \pm 0.60$ for the axis A and -0.02 ± 0.60 for the axis B , without significant dependence on the ϕ energy. They are statistically consistent with no spin alignment. For evaluation of the inclusive ϕ rate, therefore, it was assumed that the ϕ 's are unaligned.

For each of three energy bins, $0.075 < x < 0.15$, $0.25 < x < 0.40$, and $0.40 < x < 0.55$, the K^+K^- invariant-mass spectrum was fitted with a Gaussian peak at $M(K^+K^-) = 1.02$ GeV plus a background

TABLE I. The inclusive ϕ production rate normalized to the total annihilation cross section into hadrons σ_h . Here $x = 2E_\phi/\sqrt{s}$ and β is the ϕ velocity. The first error is statistical, the second is systematic.

x	$(1/\sigma_h\beta)d\sigma_\phi/dx$
0.075–0.150	$0.38 \pm 0.08 \pm 0.13$
0.250–0.400	$0.15 \pm 0.04 \pm 0.06$
0.400–0.550	$0.07 \pm 0.04 \pm 0.04$

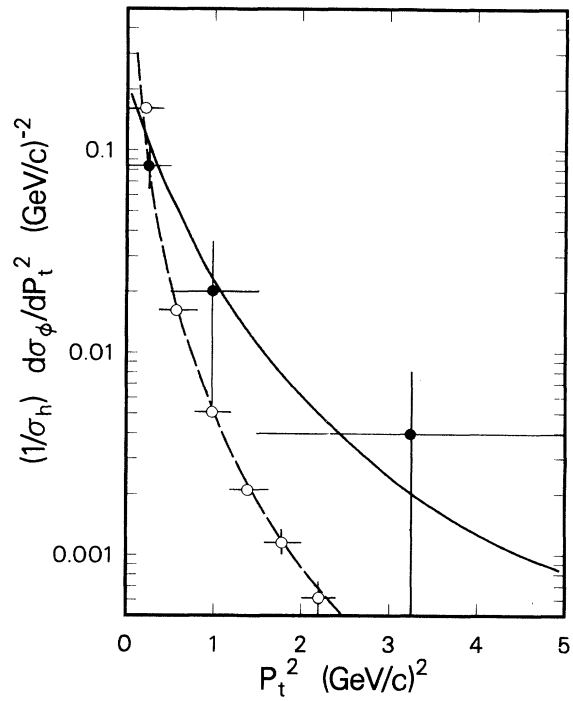


FIG. 3. Distribution of the square of the ϕ transverse momentum with respect to the thrust axis in the range $x < 0.55$ (indicated by filled circles). The open circles give the distribution observed for π^\pm scaled by a factor of $1/140$ for comparison. The horizontal bars are drawn to indicate the range of each bin. The solid and dashed curves show predictions of the Lund model for ϕ and π^\pm (scaled by $1/140$), respectively.

whose shape was obtained by Monte Carlo and parametrized with a smooth function. Figure 2(a) and Table I show the corresponding scaled cross sections $(1/\sigma_h\beta)d\sigma_\phi/dx$, where σ_h is the total annihilation cross section into hadrons. The errors include both statistical and systematic contributions from ambiguities in particle identification, estimates of backgrounds, track acceptance, and dependence on the Monte Carlo event generator used in the efficiency calculation. Figure 2(b) shows the efficiency for ϕ detection, including the known branching ratio for $\phi \rightarrow K^+K^-$ (49.1%). The loss of efficiency in the vicinity of $x = 0.2$ results from the reduced kaon acceptance due to π - K overlap in dE/dx .

By interpolating the cross section with an exponential curve in the region between the first and second bins in Fig. 2(a), we obtain $0.077 \pm 0.012(\text{stat}) \pm 0.016(\text{syst})$ ϕ 's per event for $0.075 < x < 0.55$. The smooth line in Fig. 2 shows a prediction of the Lund Monte Carlo program,⁸ obtained with $s/u = 0.3$ and $V/(V+P) = 0.5$, which is consistent with our measurement. Here s/u is the

Investigations on Scaling and Hyperscaling for Invasion Percolation

Jorge F. Willemsen

Schlumberger-Doll Research, Ridgefield, Connecticut 06877

(Received 31 October 1983)

Invasion-percolation observables which should scale with exponents interrelated through scaling and hyperscaling hypotheses are investigated. Evidence is presented that the hyperscaling relation between τ , the spatial dimension, and the fractal dimension breaks down at the defender threshold. Thus an independent exponent must be introduced to describe the scaling of the finite-defender-cluster distribution.

PACS numbers: 05.60.+w, 05.40.+j, 05.70.Jk

Invasion percolation (IP) is a dynamic process in which a cluster grows into a sample through selection of paths of least resistance.¹⁻³ The resistances to invasion are assigned randomly to the sites (or bonds) of a regular lattice, and are held fixed throughout the process. The defender is treated as an "incompressible fluid": Once it has been surrounded the invader cannot penetrate it further. There can then exist two critical points in the process. The first, or "breakthrough," point is the point at which the invader first crosses the lattice. The second, "terminal," critical point occurs when the defender has been completely disconnected into finite clusters; for this to happen it is essential that a "semipermeable wall" enclose the system, so that the defender may escape the region but the invader may not. While in $d=2$ dimensions the terminal point is identical to the breakthrough point,³ for $d \geq 3$ the two critical points are substantially different.

It is useful to analyze IP by drawing analogies with ordinary percolation. For example, the fraction of sites occupied by the invader at breakthrough, $S(L)$, scales as^{1,3} $S(L) = S_0 L^{-(d-D_I)}$, where L is the linear size of the lattice in units of the lattice spacing, and D_I is the invader fractal dimension. Further, there is an independent exponent analogous to a thermal exponent which describes the behavior of the acceptance fraction of invaded sites.^{2,3}

For ordinary percolation a powerful scaling formalism exists which relates scaling exponents of observables to two independent exponents.⁴ However, no such formalism exists for IP, so that no "proofs" of relationships among IP exponents exist at present. But as was noted in Ref. 3, one may hunt about and discover relations intrinsic to the model (purely geometrical) which are satisfied at each of the critical points. In this Letter I report on several such relationships for geometric exponents in IP.

The present results indicate that at breakthrough the fractal dimension is sufficient to quantify IP

scaling observables, as in ordinary percolation. But at the terminal critical point it appears necessary to introduce a new independent exponent. It was reported in Ref. 3 that at the terminal threshold the number of defenders in clusters containing s sites, $n(s)$, scales with s according to the power law $n(s) \approx s^{-\tau}$. (The exponent τ is meaningless for IP at breakthrough for $d=3$.) With the present data set, I find a least-squares fit⁵ $\tau = 2.05 \pm 0.04$. Now, in ordinary percolation the relation $\tau = 1 + d/D_I$ follows from hyperscaling.⁴ To test such a relation for IP, I introduce a defender fractal dimension D_S at the terminal point, and find that $D_S \neq D_I$. I then ask if τ satisfies the hyperscaling relation using D_S . The relation might hold because it encapsulates a statement about how the finite clusters are distributed in space, i.e., self-similarity under scale transformations in the precise way to be described in Eq. (3). But I find the the relation does not hold, and thus learn that the self-similarity of the clusters occurs with a characteristic dimension different from the spatial dimension.

We now discuss breakthrough in detail. As is conventional,⁶ introduce the local density $\rho(\vec{x}) = 1$ if \vec{x} is occupied by the invader; $\rho(\vec{x}) = 0$ otherwise. The scaling of the invader saturation suggests we assign the scaling dimension $D_I - d$ to the field ρ . Then the autocorrelation function

$$C(\vec{r}, L) = L^{-d} \sum_{\vec{x}} \rho(\vec{x}) \rho(\vec{x} + \vec{r})$$

should scale as $C(r, L) = L^{-2(d-D_I)} f(r/L)$ for $L > r \gg 1$. The replacement of \vec{r} by $r = |\vec{r}|$ follows from $xy(z)$ invariance, which is easily verified in the model. (This invariance basically reflects the statistical isotropy of laying the random numbers on the sites of the lattice at the outset.)

Next, introduce the conditional probability that a site a distance r away from an occupied site is also occupied, $\sigma(r, L) = C(r, L)/S(L)$. From this construct the "partial saturations"

$$S(r, L) = r^{-d} \int_0^r dx x^{(d-1)} \sigma(x, L). \quad (1)$$

We shall say that an invader cluster is a convention-